Effect of gravity on the orientation and detachment of cubic particles adsorbed at soap film or liquid interfaces

I.T. Davies[1] and C. Raufaste[2,3]

[1]Department of Mathematics, Aberystwyth University, Aberystwyth, Ceredigion SY23 3BZ, UK.
[2]Université Côte d'Azur, CNRS UMR 7010, Institut de Physique de Nice, Parc Valrose, 06100 Nice, France.
[3]Institut Universitaire de France (IUF), 75005 Paris, France.

Abstract

We investigate the interaction that occurs between a light solid cube falling under gravity and a horizontal soap film that is pinned to a circular ring. We observe in both experiments and quasi-static simulations that the final orientation of a cube that becomes entrapped by a soap film is strongly dependent on the Bond number. A cube is rotated by a soap film into one of three main orientations in a process that is driven by energy minimisation. The likelihood of observing each of these final orientations is shown to depend on the Bond number, and the most energetically favourable orientation depends on the terminal height reached by the cube. We also find a critical value for the Bond number, above which a cube is no longer supported by a soap film and detachment occurs, to be less than one.

1 Introduction

Aqueous foams are complex two-phase materials consisting of gas bubbles, liquid films and channels [1]. The interaction between a soap film and a solid object or between particles and an aqueous foam is important in froth flotation for mineral separation, paper deinking, waste water treatment and soil remediation [2, 3, 4, 5, 6]. The efficiency of the flotation process depends on the interaction that occurs between a foam's films and the particles it needs to carry and those it needs to leave behind. Experiments and a simple scaling argument show that the energy required for a particle to pass through a film scales as γr^2, the typical excess of energy due to the interface deformation, with γ the surface tension of the gas-liquid interfaces and r the radius of the object [7]. More recently, foams have found applications in microfluidics, where capillary forces tend to dominate and gravitational effects become negligible [8, 9]. The interaction that occurs between a foam's films and a solid object or particle also has many potential applications at this scale, for example in pharmaceuticals and medicine, where controlled transportation of particles, objects or solvents through confined geometries is needed [10] or where a liquid filter is needed [11].

In another context, capillary forces are key elements in patterning assemblies of nanoparticles at liquid interfaces [12, 13, 14, 15, 16], which provide materials with peculiar optical and electronic properties. For instance nanocubes self-assemble into graphenelike honeycomb and hexagonal lattices [17, 18, 19, 20] or the pattern can be tuned as the particle shape changes from a sharp cube to a rounded cube [20]. The capillary deformation induced by adsorbed cubes depends on the Young's contact angle [21, 22]. The orientation of a single cube at the interface drives the interface deformation and the arrangement. On the example of a 90° contact angle, a single-adsorbed cube prefers a configuration with one corner between three faces pointing upward, which generates a hexapolar deformation to the interface. This hexapolar deformation drives multiple cubes to self-assemble into hexagonal or graphenelike honeycomb lattices [23]. The orientation of the particles at the interface as a function of the packing, confinement and shape has attracted many studies [22, 25, 24, 26, 27, 28].

Preprint submitted to Soft Matter on 28/5/21

In both contexts, objects are considered small for gravity to be neglected. We can expect this hypothesis to fail as the size or density of the object increases. We therefore aim to provide criteria to account for gravity. We expect the relevant dimensionless quantity for cubic objects interacting with a soap film to be the Bond number $Bo = \rho g r_s^2/2\gamma$, with ρ the object density, g the standard gravitational acceleration, r_s the half side-length and γ the surface tension. (Note that ρ should be replaced by $\rho - \rho_\ell$ and 2γ by γ for the interaction at the interface of two liquids of the same density ρ_ℓ.) We have previously showed that a cube with a Bond number of 1 is reoriented by a soap film to a *flat* orientation as it descends through a horizontal soap film [29]. We now ask what are the conditions for a cubic object to be trapped or to detach from a soap film in terms of the Bond number and its initial orientation? Although we will probe the final orientation of a single cube in terms of its Bond number, this final orientation is crucial to determining the interaction between multiple cubes trapped at an interface.

In this work, we study the interaction between a soap film and a cube both in simulation and experiments. We will consider what happens when we vary the Bond number and the initial orientation of the cube systematically while the contact angle is set to 90°. We aim to probe how a cube is reoriented by a soap film it falls onto, and when does it become trapped by the soap film. In section 2, we include details of the methodology for our simulations and experiments. The result are presented in section 3 and section 4 includes our conclusions.

2 Methodology

2.1 Simulations

We use the Surface Evolver [30] to simulate the interaction between a horizontal soap film and a cube with curved corners and edges. The cube is defined by the superquadric equation

$$(x - x_0)^\lambda + (y - y_0)^\lambda + (z - z_0)^\lambda = r_s^\lambda, \tag{1}$$

where (x_0, y_0, z_0) denotes its centre of mass and r_s is the minimum distance between its centre and its surface. The shape parameter λ, which determines the curvature of the edges and corners of the cube, is kept fixed at $\lambda = 10$ throughout. The volume of the superquadric cube defined by equation (1) is calculated using the formula

$$V_s = \frac{8r_s^2}{3\lambda^2} \frac{\Gamma\left(\frac{1}{\lambda}\right)^3}{\Gamma\left(\frac{3}{\lambda}\right)} \tag{2}$$

(as derived in [31]), where the gamma functions $\Gamma(a/\lambda) = \int_0^\infty t^{a/\lambda - 1} e^{-t} dt$ are computed numerically. As in previous work [29], we set the volume of the cube to that of a sphere with radius 1, that is $V_s = \frac{4}{3}\pi$, so that its sides have a half length of $r_s \approx 0.817$. The surface area of the cube is $A_s \approx 14.24$. We vary the Bond number by varying the weight of the cube, choosing values of $Bo \in [0.1, 1.0]$.

The cube is initially positioned just above a horizontal soap film. The initial orientation of the cube is prescribed (and varied), and is described by the angles α_i between the normal vectors $\vec{N}_i$ that define it and the vertical axis, for $i = 1, 2, 3$ (see figure 1a). The boundary of the soap film is fixed on a horizontal circular ring of radius $r_c = 4$ (chosen to be large enough so that boundary effects are negligible) and height $h = 5$.

As in previous work [29], when the object is in contact with the soap film, we assume that its motion is slow and over-damped so that inertial effects can be neglected, and a quasi-static model is appropriate. In this case, the soap film is at equilibrium between small increments in the position and orientation of the cube.

The soap film exerts a network force $\vec{F}^n$ on the solid object due to the pull of surface tension, which is calculated geometrically as

$$\vec{F}^n = 2\gamma \sum_i l_i \vec{n}_i. \tag{3}$$

Here l_i denotes the contact length of the triangular facet i of the soap film that is in contact with the object and $\vec{n}_i$ denotes the unit normal vector to the surface at (x_i, y_i, z_i), the mid-point of edge i (see figure 1b),

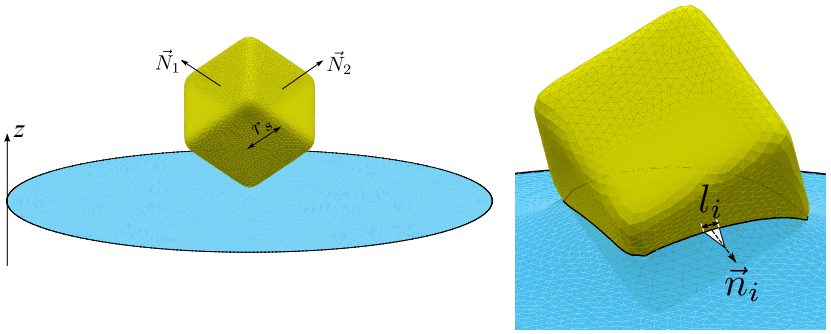

(a) (b)

Figure 1: (a) A rounded cube with side length $2r_s$ is initially positioned just above a horizontal soap film that is pinned at the boundary to a circle with radius r_c and height $z = h$. The orientation of the cube is prescribed and then traced by recording the angles that the normal vectors that define it, $\vec{N}_1$, $\vec{N}_2$ and $\vec{N}_3$ (obscured by the cube) make with the vertical axis. (b) The film exerts a network force on the cube due to surface tension; for each edge i of the triangulated surface of the soap film that contacts the cube, an outward network force is exerted in the normal direction, $\vec{n}_i$ over its length l_i.

and 2γ is the surface tension of the film (which we set to 1 in our simulations). Since the surface of the film contacts the object at 90°, it applies a network torque, $\vec{\tau}^n$:

$$\vec{\tau}^n = 2\gamma \sum_i l_i \vec{r}_i \times \vec{n}_i, \tag{4}$$

where $\vec{r}_i = (x_i - x_0, y_i - y_0, z_i - z_0)$ is the vector that connects the centre of the object with the midpoint of edge i. Therefore the force on the cube is

$$\vec{F} \quad = \quad -mg\vec{z} + \vec{F}^n \tag{5}$$

where $\vec{z}$ denotes the unit vector in the positive z direction.

At each time step of a simulation, the soap film is equilibrated while the position and orientation of the cube is fixed. The cube is then moved by $\varepsilon\vec{F}$ and rotated it by $\varepsilon\vec{\tau}$ where ε is a small parameter that sets the effective time scale of the simulations. We choose $\varepsilon = 2.5 \times 10^{-3}$ throughout this work. The soap film is then re-equilibrated and the process is repeated.

The equilibrium states are found by minimizing the energy of the film, which is proportional to its surface area A, using gradient descent and conjugate gradient iterations. Our energy minimization procedure continues until convergence of the energy E to within a tolerance of 1×10^{-5} has been achieved, which can take up to 10,000 iterations. The iterations are interspersed with upkeep of the tessellation and checks for soap film detachment. We also apply small perturbations to the surface of the soap film during the equilibration process by jiggling the vertices slightly. In this case, a random displacement is applied to each vertex independently using a Gaussian distribution with a deviation of 0.02 times the mean edge length of the triangular mesh [30]. This perturbation was found to be robust enough to optimize the process of reaching a minimum energy for the soap film under the given constraints.

2.2 Experiments

Soap films are formed from a SLES/CAPB/SLES mixture [32]: we mixed 6.6% of sodium lauryl ether sulfate (SLES) and 3.4% of cocamidopropylbetaine (CAPB) in mass in ultrapure water; we then dissolved 0.4% in mass of myristic acid (MAc), by stirring and heating at 60°C for one hour, and we diluted 20 times this solution with water. The surface tension of the final solution equals 23.8 mN.m^{-1}. This solution is known for its high dissipative properties [33] which prevent any significant flow from the film to the meniscus at the contact with the object at the time scale of one experiment.

A second solution was obtained by dissolving tetradecyl trimethyl ammonium bromide (TTAB) into deionizedwater. The concentration in TTAB was 3 g/l for the aqueous solution and the surface tension equals 38 mPa.m [34, 35].

In both solutions a small quantity of fluorescein sodium salt (0.5 g/L) was added for better visualization. The soap films are formed and held on a circular wire, 8 cm in diameter.

Cubes are 3D printed in polylactic acid (PLA) with a radius ranging between 0.5 and 2.8 mm. The density of PLA is 1.25 g.cm^{-3}. This leads to Bond numbers between 0.06 and 1.9. Cubes are initially pre-wetted and are held with tweezers at the contact with the soap film or slightly above it. For each cube, 10 experiments are performed with various initial orientations. Once the cubes are released, the dynamics is recorded with a color highspeed camera at 50-500 frames per second.

3 Results

In this section, we present results from simulations and experiments. First we investigate the final orientation of a cube that is trapped by a soap film and how this varies with the Bond number. We go on to determine the critical value of the Bond number for which a cube detaches from a soap film and continues its descent under gravity. Throughout this section, we will refer to three main (stable or meta-stable) orientations for a cube in contact with a soap film: (i) a *flat orientation*, where one of the angles α_i is zero and the other two are equal to $\pi/2$, (ii) a *diagonal orientation* in which two of the angles are equal to $\pi/4$ and the other is $\pi/2$, and (iii) a *rotated orientation* where all three angles are equal. We will from now on refer to orientations (i)-(iii) as $\{100\}$, $\{110\}$ and $\{111\}$ respectively.

In simulations, we varied the initial orientation of the cube as well as the Bond number. We set the initial orientation of the cube by rotating it around the x-axis by an angle $n\pi/10$, and then around the y-axis by $m\pi/10$, considering all possible combinations of $n, m \in \{0, 1, .., 5\}$. We vary the Bond number between 0.1 and 1.

Figure 2 includes snapshots from three simulations that show how the orientation of a cube changes over time as it interacts with a soap film. The initial orientation of the cube is the same for the three simulations shown, while the Bond numbers are $Bo = 0.1$, 0.375, 0.5. The cube becomes trapped by the soap film in all three cases, but its final orientation varies with the Bond number. The cube settles into the $\{111\}$, $\{110\}$ and $\{100\}$ orientations in order of increasing Bond numbers. We will try to explain this surprising result later, but let us first investigate whether or not the final orientation of a cube that becomes entrapped by a soap film is independent of its initial orientation.

We investigate how the orientation of a cube that becomes entrapped by a soap film varies from all initial orientations considered in our simulations. Figure 3a shows that the most likely settling orientation for a cube with Bond number $Bo = 0.375$ is the $\{111\}$ orientation. In this case, the cube only settles into the $\{110\}$ or $\{100\}$ orientations when the initial orientations are very close to these (as shown in figure 2). For a Bond number of $Bo = 0.25$ (data not shown), we observed that a cube rotates to the $\{111\}$ orientation unless it is initially very close to the $\{100\}$ orientation. When $Bo = 0.1$, a cube always rotated to the $\{111\}$ orientation, even when it started from the $\{100\}$ orientation. Figure 3b shows that a cube with Bond number $Bo = 0.5$ always rotated to the $\{100\}$ orientation. This is also the most likely final orientation for cubes with a higher Bond number, even those that detach from a soap film, as shown in previous work [29]. The final orientation of a cube that interacts with a horizontal soap film versus the Bond number is summarised in full in figure 4.

We find a critical value of the Bond number, denoted Bo_c, for which a cube's weight is no longer supported by the soap film and detachment occurs. In simulations, we found that a cube with Bond number 0.6 was trapped by the soap film, while a cube with a Bond number of 0.7 was not supported and detached from the soap film. We therefore extrapolate that the critical value of the Bond number is $Bo_c = 0.65 \pm 0.05$ in simulations (as shown in figure 4).

We now seek to validate these results on the final orientation of an entrapped cube as well as the critical value of the Bond number by comparing with experiments.

First we present the results with the SLES/CAPB/SLES solution. In experiments the Bond number is varied between 0.06 and 1.9 and we focus on the range of interest in figure 5. Only two stable configurations

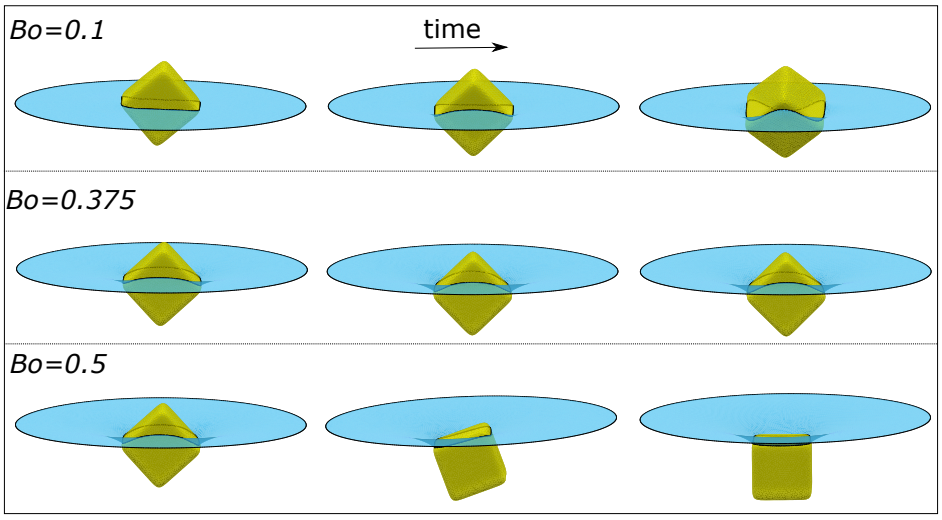

Figure 2: Snapshots from simulations in which a cube, with an initial orientation that is just off the {110} orientation (with $\alpha_1 = \pi/2$, $\alpha_2 = \pi/5$ and $\alpha_3 = 4\pi/5$), interacts with a soap film for Bond numbers $Bo = 0.1$, 0.375, 0.5. The snapshots in the left column are taken after 200 time steps, while the centre and right columns are after 500 and 1,000 time steps respectively. The right column represents the final position of the cubes.

are observed. For $0.06 \leq Bo \leq 0.25$, the {111} orientation is systematically observed, but we noticed that the {110} orientation can appear transiently (Movie 1 in the Supplemental Material). For $Bo = 0.38$ both the {111} and the {100} orientations were observed, which indicates a significant change around this value in agreement with simulation. For $Bo = 0.55$, only the {100} orientation is observed, but the cube detaches in some cases. This value of the Bond number corresponds to the entrapment/detachment transition in experiments and the cube detaches systematically for larger Bo (Movie 2 in the Supplemental Material). This value for the critical Bond number is slightly lower than $Bo_c \approx 0.65$ found in simulations. This lower value can be attributed either to the small amount of liquid that collects on the lower surface of a cube in experiments, thus contributing to an additional weight that is not accounted for by the Bond number, or to the inertia of the object that is neglected in the model.

A second round of experiments were performed with the TTAB solution. Here we observe a flow from the soap film to the meniscus due to capillary suction [36]. This flow makes a difficult comparison between experiments and simulations since the later assume an infinitely small meniscus. As an example in figure 6, $Bo = 0.24$ should lead to the diagonal configuration as expected from the first set of experiment with the SLES/CAPB/SLES solution and from the simulations. This is indeed observed initially, but after a few seconds the growing meniscus triggers a transition toward a flat orientation with the bottom/top side of the meniscus connecting the bottom/top side of the cube respectively. This shows that the notion of final orientation depends on the timescale considered: it depends on the time it takes for the liquid to rearrange inside the soap film and the meniscus. As observed, this dynamics is strongly correlated with the nature of the surfactant solution.

We now return to simulations to discuss the multiple scenarios at play in more detail. To explain why a cube with a given Bond number is rotated to a particular final orientation by a horizontal soap film, we consider how the energy of the soap film varies in our simulations. Figure 7a shows how the energy of the film varies with the height of the descending cube. The data shown here is for Bond numbers ranging between 0.1 and 0.75, with the cube initially oriented in the {100}, {110} or {111} orientations. The energy is given in terms of a dimensionless absorption energy per unit area, $E_1/2\gamma A_s$, where $E_1 = 2\gamma(A - \pi r_c^2)$ is the difference between the energy of the soap film in its current state and at an unperturbed state. As already noted, a cube with $Bo = 0.75$ is too heavy to become entrapped by the soap film, but it is also not reoriented by the soap film from any of these three main orientations. This is shown by the three distinct curves labeled A, B and C in figure 7a. A drop in the surface energy occurs when the cube touches and perturbs the soap

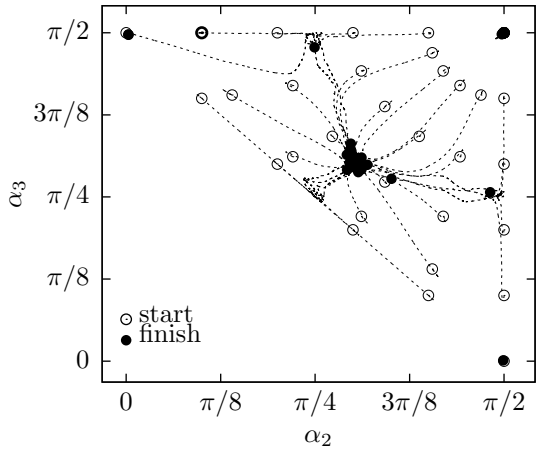

(a)

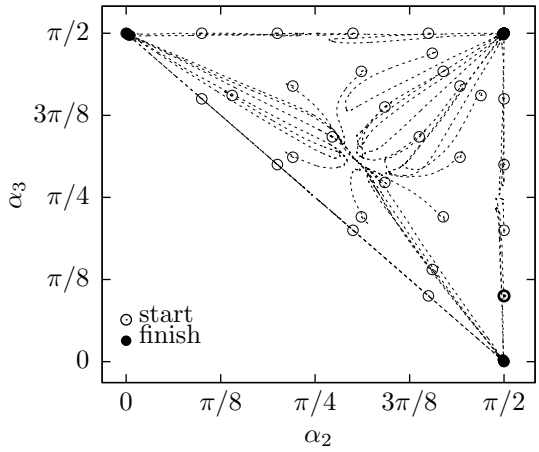

(b)

Figure 3: The orientation of a cube with (a) $Bo = 0.375$ and (b) $Bo = 0.5$, given in terms of the angles (α_2, α_3), is tracked over time from all initial orientations considered in our simulations. Note that the pairwise angles $(0, \pi/2)$, $(\pi/2, \pi/2)$ and $(\pi/2, 0)$ represent the $\{100\}$ orientation here, $(\pi/4, \pi/2)$ and $(\pi/2, \pi/4)$ both denote the $\{110\}$ orientation, and the $\{111\}$ orientation is given by $\left(\tan^{-1}\left(1/\sqrt{2}\right), \tan^{-1}\left(1/\sqrt{2}\right)\right)$.

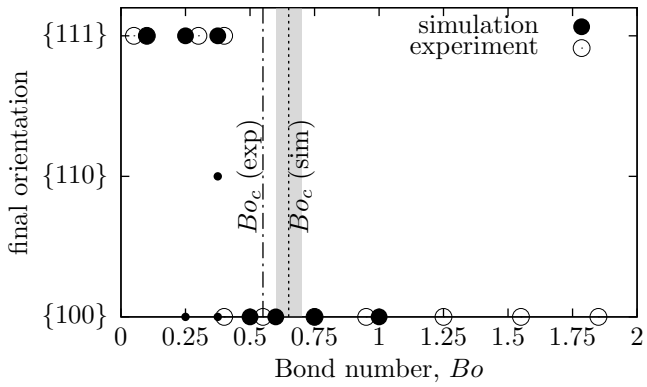

Figure 4: The final orientation of a cube interacting with a horizontal soap film versus the Bond number, for simulation and experiments. The vertical lines denote the critical value of the Bond number (Bo_c) found in simulations and experiments, above which a cube detaches from the soap film. The shaded region indicates an error bar of ± 0.05. For simulations, the large markers indicate the most likely final orientation for a cube for a particular Bond number, while the small markers indicate final orientations that are observed but which are much less likely.

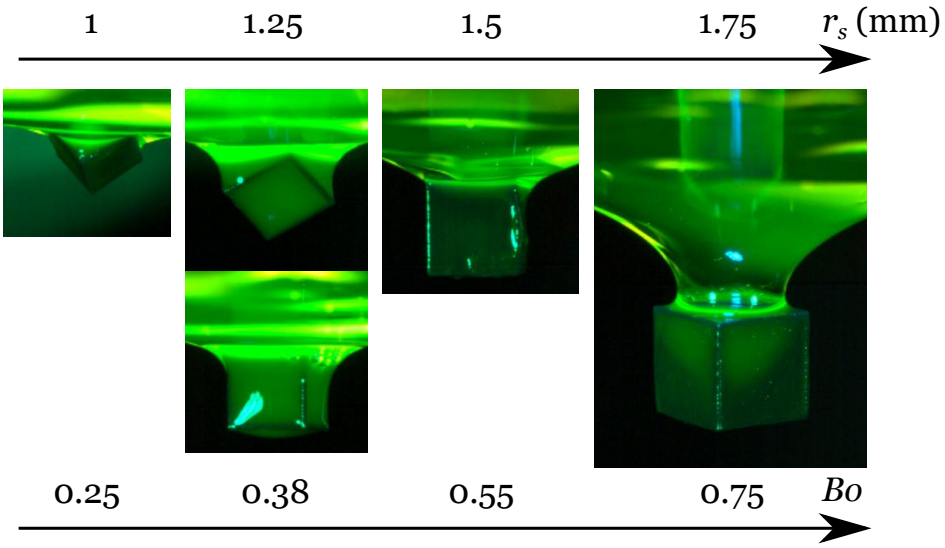

Figure 5: Stable or transient orientations for various Bo in the range 0.2 - 0.8 found in experiments.

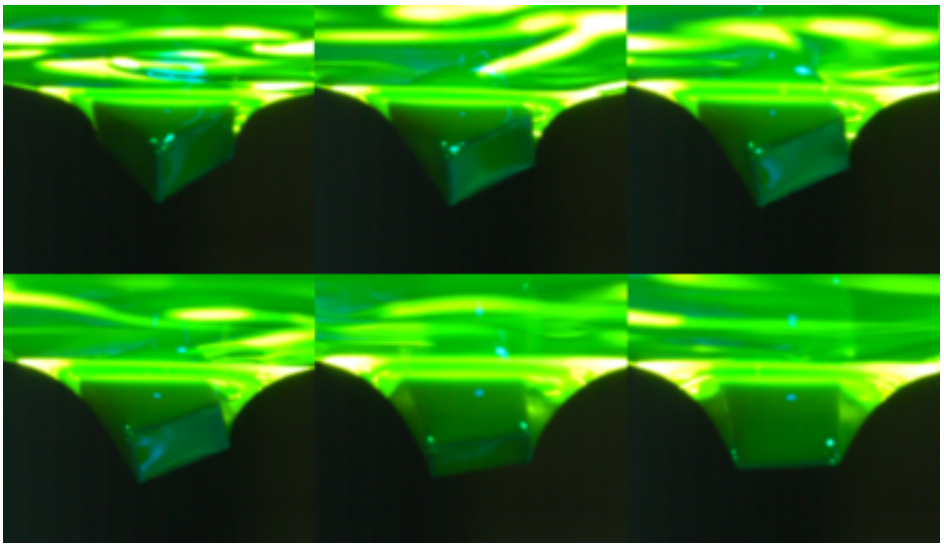

Figure 6: Evolution of the orientation due to the growth of the meniscus. TTAB solution, $r_s = 1.25$, $Bo = 0.24$, 5 s between the first and last images (Movie 3 in Supplemental Material).

film for the first time, and the energy continues to decrease to a minimum when the height of the cube is perfectly aligned with the height at which the outer boundary of the soap film is pinned. At this point, the energy of the soap film is at its lowest for the cube in the {111} orientation. Once the cube has passed this point, the surface energy increases as the film becomes stretched, before the cube eventually detaches from the soap film. The film is stretched the most before detachment for the cube in the {100} orientation.

It can be seen in figure 7a that a cube with $Bo \leq 0.5$ can be rotated by a soap film from one metastable orientation to a more energetically favourable orientation. This is shown by the jumps from one of the distinct energy curves (labelled A, B and C) to another. These transitions are surprising given the symmetric deformation caused to the soap film by each of the three main orientations. They are triggered by small imperfections in our mesh approximation of the structure. The orientation of an entrapped cube that results in perturbing the soap film so that its energy is minimised is dependent on the height reached by the cube, which in turn depends on the initial orientation of the cube and the Bond number. If the centre of the cube has advanced less than r_s past the height h at which the film is pinned at the boundary, then it is almost always rotated by the soap film to the {111} orientation, which is the orientation that achieves the minimum energy for the soap film here. The stability of the {100} and {110} orientations decreases with the Bond number, and as a result a cube with $Bo = 0.1$ is rotated from both of these orientation into the stable {111} orientation. If a cube advances beyond this height, then it is always rotated by the soap film to the {100} orientation, which results in the most energetically favourable perturbation of the soap film here. It is interesting to note what happens when the settling position of the cube is very close to $h - r_s$, as happens in a couple of simulations where $Bo = 0.375$. The three energy curves in figure 7a intersect here, thus the three main orientations are as energetically favourable as each other at this point. This explains why a cube with this Bond number can settle on the soap film with the {110} orientation from a similar initial orientation (as seen in figure 2).

In a second set of simulations we probe the stability of the three main final orientations in the trapped regime. At mechanical equilibrium, we have that $\vec{F} = \vec{0}$ in Eq. (5), from which we can write the equilibrium Bond number $Bo_{eq} = F_z^n r_s^2/(2\gamma V_s)$. Thus measuring the vertical component F_z^n of the drag force exerted by the film gives a direct measurement of the Bond number of the trapped object. For each (fixed) orientation, the object is artificially displaced through the soap film from first contact to detachment to sweep all the possible combinations of Bond numbers and surface energies. Figure 7b shows how the energy of the soap film varies with Bo_{eq} for the three main cube orientations. This confirms that the orientation {111} is the most energetically favourable when the Bond number is small and that only the {100} orientation is achievable when the Bond number is greater than 0.5 with a critical Bond number around 0.69 that gives

the maximal value before detachment. The {110} orientation is never optimal in terms of perturbing the soap film in a way that achieves a minimum energy. Note that for a given Bond number, there exists two branches for orientations {111} and {110} and only the lower one is stable.

4 Discussion and conclusions

We have observed in both simulations and experiments that the final orientation of a cube that becomes entrapped by a soap film depends on the Bond number, which determines the settling height of the cube. A light cube with a Bond number $Bo < 0.375$ becomes entrapped by a soap film and is almost always rotated to the {111} orientation. For these Bond numbers, a cube descends less than half its side length past the height of the soap film, and in this range it is the {111} orientation for the cube that perturbs the soap film so that its energy is minimized. A cube with a Bond number $Bo \approx 0.375$ is almost always rotated to the {111} orientation as before. However if the cube has an initial orientation that is very close to either the {110} or {100} orientations, then it will rotate into the nearest of these orientations. The {110} orientation was rarely observed for other Bond numbers. This special case can be explained by the fact that the absorption energy of the soap film is very similar for all three cube orientations for $Bo = 0.375$. For larger Bond numbers, a cube that becomes entrapped in the soap film is always rotated to the {100} orientation, which provides the minimum energy for the soap film when the cube has descended well beyond the height of the soap film. These results should help in patterning capillary assemblies with prescribed orientations. Orientation {111} is quite easily obtained as long as objects are light enough. On the opposite, observing the {100} orientation would require a precise control of the Bond number, between 0.5 and 0.65, while the {110} orientation would be almost impossible to obtain in a controlled way.

We found that the critical Bond number (Bo_c), above which a cube is no longer supported by a soap film, is less than one. This can be explained by a simple force balance argument. From our results, we know that the maximum drag force applied by a soap film on a cube occurs when the cube is in the {100} orientation and the film contacts it over its upper horizontal face, forming a stretched catenoidal neck (as seen in figure 5). The catenoidal shape of the soap film means that the contact with the cube is well approximated by a circle. For a cube with sharp edges and corners, the largest circle that can be inscribed onto this surface has radius r_s, and since we assume that the soap film meets the obstacle at 90°, an upper bound for the network force is given by $4\pi r_s\gamma$. Balancing this out with the weight (mg) of the cube gives an approximation of the critical Bond number of

$$Bo_c = \frac{mgr_s^2}{2\gamma V_s} \approx \frac{(4\pi r_s\gamma)r_s^2}{2\gamma V_s} = \frac{2\pi r_s^3}{V_s} \approx 0.82.$$

This approximation can be improved if we also take into account the curved edges and corners of the cubes that we used. This reduces the size of the largest circle that can be inscribed into the horizontal region of the upper surface of the cube. For the superquadric definition that we used for the cube (in equation 1), with $\lambda = 10$, a horizontal plane $z = z_0 + r_s$ approximates the upper surface of the cube (to within 1% accuracy) over a diameter of $1.5r_s$. Therefore our estimate for the critical Bond number reduces to $Bo_c = 1.5\pi r_s^3/V_s \approx 0.61$, which is similar to what we observed in our simulation and experiments.

In our simulations, we kept the contact angle between the soap film and the cube fixed at 90°, as this provided a reasonable approximation for what we observed in experiments as long as the dynamics is quasistatic [37, 38]. This contact angle is clearly an important parameter, and changing it will surely affect the final orientation of entrapped cubes, as already observed in the small Bo limit [21, 22], as well as the value of the critical Bond number Bo_c. For instance, we predict that decreasing the contact angle (meaning the liquid on top has a larger affinity with the object than the liquid at the bottom in the case of an interface between two liquids) will increase the value of the critical Bond number (Bo_c), but it is not clear what would become the most dominant final orientation of a cube as it becomes entrapped by a soap film. We did not consider in detail what happens when a cube detaches from a soap film. We observed in experiments that bubble entrainment occurs as it does for a spherical particle [39, 40]. We expect that the size of bubbles generated during detachment will depend on the contact angle as well as the orientation and the sharpness of the edges and corners of the cube. A more detailed investigation of the effect of film thickness is also left as future work.

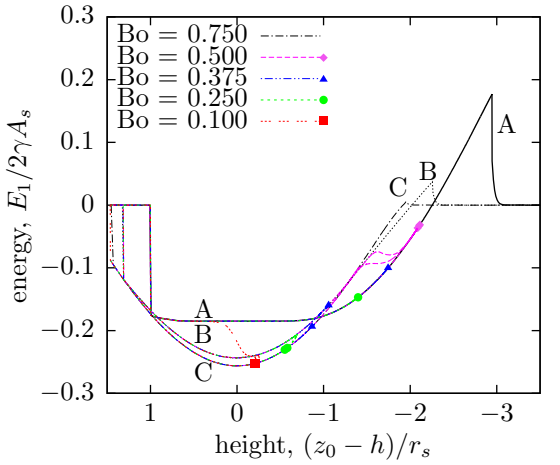

(a)

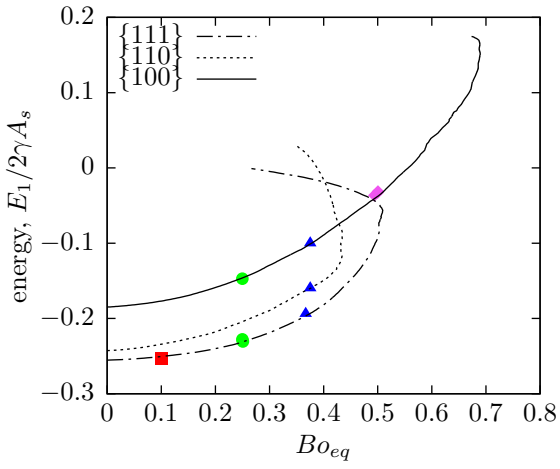

(b)

Figure 7: The variation of the dimensionless absorption energy per unit area of the soap film ($E_1/2\gamma A_s$) versus (a) the normalised height of the cube, $(z_0 - h)/r_s$, and (b) the equilibrium Bond number Bo_{eq}. In (a), cubes of different Bond numbers descend (from left to right on the height-axis) from the three main orientations {100}, {110} and {111}, labelled A, B and C respectively. The markers denote the settling position of a cube that becomes entrapped by the soap film. In (a) and (b), trajectories obtained for the three main orientations {100}, {110} and {111} if fixed are displayed as black solid, dotted and dash-dotted lines respectively. In (b) the markers of the final orientations obtained in (a) are represented too.

Finally, we note a fundamental difference between cubes at the interfaces of a soap film and at the interface between two immiscible liquids. In the former case the presence of a meniscus can trigger effects that are not accounted for by our model. As emphasized with experiments, a meniscus triggers a flow, with a speed that depends on the nature of the surfactant and on the viscosity of the solution. At a large time scale we can expect the width of the meniscus to be comparable to the size of the cube, and a change of orientation for the cube is possible. Conversely, capillary assemblies at the interface between two immiscible liquids should be stable with respect to this process.

Conflicts of interest

There are no conflicts to declare.

Acknowledgments

We thank Simon Cox for stimulating discussions and Ken Brakke for developing and maintaining the Surface Evolver. TD acknowledges Supercomputing Wales facilities. CR acknowledges support by the French government, through the National Research Agency (ANR-20-CE30-0019) and through the UCA$^{\text{JEDI}}$ Investments in the Future project of the National Research Agency (ANR-15-IDEX-01).

References

[1] I. Cantat, S. Cohen-Addad, F. Elias, F. Graner, R. Höhler, O. Pitois, F. Rouyer, and A. Saint-Jalmes. *Foams Structure and Dynamics*. Oxford University Press, 2013.

[2] R. K. Prud'homme and G. G. Warr. Foams in mineral flotation and separation processess. In R. K. Prud'homme and S. A. Khan, editors, *Foams: Theory, Measurements and Applications*. CRC Press, 1996.

[3] B.J. Shean and J.J. Cilliers. A review of froth flotation control. *International Journal of Mineral Processing*, 100:57 – 71, 2011.

[4] D. Feng and A. V. Nguyen. Effect of contact angle and contact angle hysteresis on the floatability of spheres at the air-water interface. *Advances in colloid and interface science*, 248:69–84, 2017.

[5] Y. Xing, X. Gui, L. Pan, B. Pinchasik, Y. Cao, J. Liu, M. Kappl, and H. Butt. Recent experimental advances for understanding bubble-particle attachment in flotation. *Advances in colloid and interface science*, 246:105–132, 2017.

[6] F. Schellenberger, P. Papadopoulos, M. Kappl, S. Weber, D. Vollmer, and H. Butt. Detaching microparticles from a liquid surface. *Physical Review Letters*, 121:048002, 2018.

[7] A. Le Goff, L. Courbin, H. A. Stone and D. Quéré. Energy absorption in a bamboo foam. *EPL*, 84:36001, 2008.

[8] A. Huerre, V. Miralles, and M-C. Jullien. Bubbles and foams in microfluidics. *Soft Matter*, 10:6888–6902, 2014.

[9] G. M. Whitesides. The origins and the future of microfluidics. *Nature*, 442:368–373, 2006.

[10] W. Drenckhan, S.J. Cox, G. Delaney, H. Holste, D. Weaire, and N. Kern. Rheology of ordered foams – on the way to discrete microfluidics. *Colloids and Surfaces A: Physicochemical and Engineering Aspects*, 263:52 – 64, 2005.

[11] B. Stogin, L. Gockowski, H. Feldstein, H. Claure, J. Wang, and T. Wong. Free-standing liquid membranes as unusual particle separators. *Science advances*, 4(8):eaat3276, 2018.

[12] R. Di Leonardo, F. Saglimbeni, and G. Ruocco. Very-Long-Range Nature of Capillary Interactions in Liquid Films. *Phys. Rev. Lett.*, 100:106103, 2008.

[13] L. Yao, L. Botto, M. Cavallaro Jr, B. J. Bleier, V. Garbin, and K. J. Stebe. Near field capillary repulsion/ *Soft Matter*, 9:779–786, 2013.

[14] R. McGorty, J. Fung, D. Kaz, and V. N. Manoharan. Colloidal self-assembly at an interface. *Materials Today*, 13(6):34–42, 2010.

[15] E. M. Furst. Directing colloidal assembly at fluid interfaces. *Proceedings of the National Academy of Sciences*, 108(52): 20853–20854, 2011.

[16] A. D. Law, M. Auriol, D. Smith, T. S. Horozov, and D.M.A. Buzza. Self-Assembly of Two-Dimensional Colloidal Clusters by Tuning the Hydrophobicity, Composition, and Packing Geometry. *Phys. Rev. Lett.* 110, 138301, 2013.

[17] W. H. Evers, B. Goris, S. Bals, M. Casavola, J. de Graaf, R. van Roij, M. Dijkstra, and D. Vanmaekelbergh. Low-Dimensional Semiconductor Superlattices Formed by Geometric Control over Nanocrystal Attachment. *Nano Lett.*, 13(6): 2317–2323, 2013.

[18] M. P. Boneschanscher, W. H. Evers, J. J. Geuchies, T. Altantzis, B. Goris, F. T. Rabouw, S. A. P. van Rossum, H. S. J. van der Zant, L. D. A. Siebbeles, G. Van Tendeloo, I. Swart, J. Hilhorst, A. V. Petukhov, S. Bals, and D. Vanmaekelbergh. Long-range orientation and atomic attachment of nanocrystals in 2D honeycomb superlattices. *Science*, 344:1377–1380, 2014.

[19] W. Beugeling, E. Kalesaki, C. Delerue, Y.-M. Niquet, D. Vanmaekelbergh, and C. Morais Smith. Topological states in multi-orbital HgTe honeycomb lattices. *Nat Commun*, 6:6316, 2015.

[20] D. Wang, M. Hermes, R. Kotni, Y. Wu, N. Tasios, Y. Liu, B. De Nijs, E. Van Der Wee, C. Murray, M. Dijkstra, et al. Interplay between spherical confinement and particle shape on the self-assembly of rounded cubes. *Nature communications*, 9(1):1–10, 2018.

[21] G. Morris, S.J. Neethling, and J.J. Cilliers, Modelling the self orientation of particles in a film, *Minerals Engineering*, 33:87–92, 2012.

[22] E. L. Sharp, H. Al-Shehri, T. S. Horozov, S. D. Stoyanov, and V. N. Paunov. Adsorption of shape-anisotropic and porous particles at the air–water and the decane–water interface studied by the gel trapping technique. *RSC Adv.*,4:2205–2213, 2014.

[23] G. Soligno, M. Dijkstra, and R. van Roij. Self-assembly of cubes into 2d hexagonal and honeycomb lattices by hexapolar capillary interactions. *Phys. Rev. Lett.*, 116:258001, 2016.

[24] G. Soligno, M. Dijkstrab, and R. van Roija. Self-assembly of cubic colloidal particles at fluid–fluid interfaces by hexapolar capillary interactions. *Soft Matter*, 14:42–60, 2018.

[25] T. G. Anjali, and M. G. Basavaraj Shape-Induced Deformation, Capillary Bridging, and Self-Assembly of Cuboids at the Fluid–Fluid Interface. *Langmuir*, 33(3): 791–801, 2017.

[26] Q. Song, and H. Schönherr. Control of Orientation, Formation of Ordered Structures, and Self-Sorting of Surface-Functionalized Microcubes at the Air–Water Interface. *Langmuir*, 35(20):6742–6751, 2019.

[27] Q. Song, M. Zuo, and H. Schönherr. Reconfigurable Microcube Assemblies at the Liquid/Air Interface: The Impact of Surface Tension on Orientation and Capillary-Force-Interaction-Driven Assembly. *Langmuir*, 35(24):7791–7797, 2019.

[28] C. Anzivino, G. Soligno, R. van Roij, and M. Dijkstra. Chains of cubic colloids at fluid-fluid interfaces. *Soft Matter*, 17:965, 2021.

[29] I.T. Davies. Simulating the interaction between a descending super-quadric solid object and a soap film. *Proceedings of the Royal Society A: Mathematical, Physical and Engineering Sciences*, 474(2218):20180533, 2018.

[30] K. Brakke. The Surface Evolver. *Exp. Math.*, 1:141–152, 1992.

[31] A. Jaklic, A. Leonardis, and F. Solina. *Segmentation and Recovery of Superquadrics*, volume 20, chapter Superquadrics and Their Geometric Properties, pages 13–39. Springer Science and Business Media, 2000.

[32] K. Golemanov, N. D. Denkov, S. Tcholakova, M. Vethamuthu, and A. Lips, Surfactant Mixtures for Control of Bubble Surface Mobility in Foam Studies, Langmuir 24, 9956–9961 (2008).

[33] N. D. Denkov, S. Tcholakova, K. Golemanov , K. P. Ananthpadmanabhan and A. Lips, The role of surfactant type and bubble surface mobility in foam rheology, Soft Matter 5, 3389–3408 (2009).

[34] A. Cohen, N. Fraysse, J. Rajchenbach, M. Argentina, Y. Bouret, and C. Raufaste, Inertial Mass Transport and Capillary Hydraulic Jump in a Liquid Foam Microchannel, Phys. Rev. Lett. 112, 218303 (2014).

[35] A. Cohen, N. Fraysse, and C. Raufaste, Drop coalescence and liquid flow in a single Plateau border, Phys. Rev. E 91, 053008 (2015).

[36] A. A. Sonin, A. Bonfillon, and D. Langevin, Role of surface elasticity in the drainage of soap films, Phys. Rev. Lett. 71, 2342 (1993).

[37] C. Raufaste, G. Kirstetter, F. Celestini, and S. J. Cox, Deformation of a Free Interface Pierced by a Tilted Cylinder, EPL 99, 24001 (2012).

[38] C. Raufaste and S. Cox, Deformation of a Free Interface Pierced by a Tilted Cylinder: Variation of the Contact Angle, Colloids and Surfaces A: Physicochemical and Engineering Aspects 438, 126 (2013).

[39] C.H. Chen, A. Perera, P. Jackson, B. Hallmark, and J.F. Davidson. The distortion of a horizontal soap film due to the impact of a falling sphere. *Chemical Engineering Science*, 2019.

[40] S. J. Cox and I. T. Davies. Bubble entrainment by a sphere falling through a horizontal soap foam. *EPL (Europhysics Letters)*, 130(1):14002, may 2020.